

DEM RETRIEVAL AND GROUND MOTION MONITORING IN CHINA

Guido Gatti¹, Daniele Perissin², Teng Wang^{1 3} and Fabio Rocca¹

(1) *Dipartimento di Elettronica e Informazione, Politecnico di Milano, via Ponzio 34/5, 20133 Milan, Italy;*

(2) *Institute of Earth and Information Science, Chinese University of Hong Kong, Shatin, Hong Kong;*

(3) *Liesmars, Wuhan University, Luoyu Road 129, 430079 Wuhan, China*

Email: ggatti@elet.polimi.it

ABSTRACT

This paper considers the topographic measurement and analysis basing on multi-baseline Synthetic Aperture Radar data. In 2009, the ongoing works were focused on taking advantage of Permanent Scatterers (PS) Interferometry to estimate the terrain elevation and ground motion in not urban contexts. An adapted version of the method, namely Quasi-PS (QPS) technique, has been used in order to exploit the distributed target information. One of the analyzed datasets concerns the mountainous area around Zhangbei, Hebei Province, from which a geocoded Digital Elevation Model (DEM) has been retrieved. Regarding ground motion monitoring, our attention was focalized on two different areas. The first is a small area near the Three Gorges Dam, in which ground deformations have been identified and measured. The second area regards the west part of the municipality of Shanghai, centered on a straight railway. The subsidence in that zone has been measured and the interferometric coherence of the railway has been studied, according to the hypothesis of spatial and temporal stability of this kind of target.

1. INTRODUCTION

Topographic measurement is crucially important for the estimation of Digital Elevation Models (DEMs) and ground deformations monitoring. In particular, China is a huge country of which most part still needs to be precisely mapped. Land subsidence in China occurs in different regions, primarily due to groundwater withdrawal and tectonic movements. Moreover, the occurrence of landslides is largely predisposed by geological structures and topography. Nonetheless, nowadays China is in an era of rapid urbanization and infrastructure construction. Large-scale constructions needs to be continuously monitored in order to prevent hazards. As examples, Three Gorges Dam area presents a high landslides risk. The high-speed railway system needs to be carefully kept under control, since more than 80 cities in China are suffering subsidence where the railway pass [1]. However, the expenses of conventional deformation survey are not acceptable for enormous areas.

Interferometric Synthetic Aperture Radar (InSAR) data are very useful to solve the problem at hand, since the swath width of spaceborne SAR images (100km in the case of ESA ERS and Envisat) makes it possible to monitor huge areas at a time. Moreover the archives like those acquired by the European Space Agency (ESA) satellites allow recovering historical deformation time series of several years depending on the area location. The Permanent Scatter (PS) technique, developed in Politecnico di Milano in the late 1990s [2], is a well-known method to extract precise height and ground deformation estimates from interferometric data stacks. Instead of analyzing each pixel of a SAR image, PSInSAR identifies certain artificial or natural point-like stable reflectors (i.e. PS) from long series of interferometric SAR images. On such points it is possible to obtain height estimates with sub-meter accuracy and millimetric terrain motion detection [3,4]. The application of the PS-InSAR technique in urban areas has been especially studied in the past [5].

The main aim of this paper is focused on taking advantage of PS technique in order to study extra-urban contexts. As a consequence, an adapted version of the method, the Quasi-PS (QPS) technique, has been used in order to exploit the distributed target information [6,7]. The QPS technique allows the improvement of the target density, identifying and exploiting partially coherent targets, to estimate ground motions and terrain elevation where the classical PS technique fails.

This paper is organized as follows. Section 2 presents the DEM carried out from the analysis of a mountainous area around Zhangbei. Section 3 contains an analysis of ground deformation in the neighborhood of the Three Gorges Dam area. Furthermore, a validation of the QPS technique is performed comparing its results with the ones retrieved by the same dataset pre-processed by means of Singular Value Decomposition (SVD) technique. Section 4 shows the results obtained from the analysis of a straight railway located in the west part of the municipality of Shanghai. On that area both the subsidence and the interferometric coherence of the railway have been studied. Finally, conclusions are drawn in Section 5.

2. DEM RETRIEVAL BY MEANS OF QPS TECHNIQUE

One zone of interests within the Dragon 2 project is the mountainous area around Zhangbei, Hebei Province, centered at about E114.68 deg., N41.17 deg. It is well known that PS InSAR is a technique suitable to estimate the elevation and deformation of the terrain over many years and slightly different looking angles. However, point-like targets are generally present only in urban contexts. Here we present the results got in a partially vegetated area by analyzing targets that show less ideal scattering properties, using the above cited QPS technique. Starting from the knowledge of the SRTM DEM, the coherence matrix estimated from the radar images has been used to identify the information in the data-set. The heights are then retrieved in a multi-baseline framework.

Fig.1, top left, shows the reflective map (amplitude incoherent mean) calculated on the whole dataset, consisting in 12 SAR images (track 304) acquired by the ESA satellite ENVISAT in the time span from 2003 to 2009. Fig. 1, top right, shows the spatial coherence obtained averaging the coherences of a selected set of interferograms. The results of the QPS processing are displayed in the bottom left panel, in which the height error in respect to the a-priori DEM is presented. Finally, the bottom right panel of Fig.1 shows the same DEM geocoded in UTM coordinates.

The resulting DEM is very detailed, highlighting in this way the great potentiality of the QPS technique in extra-urban areas.

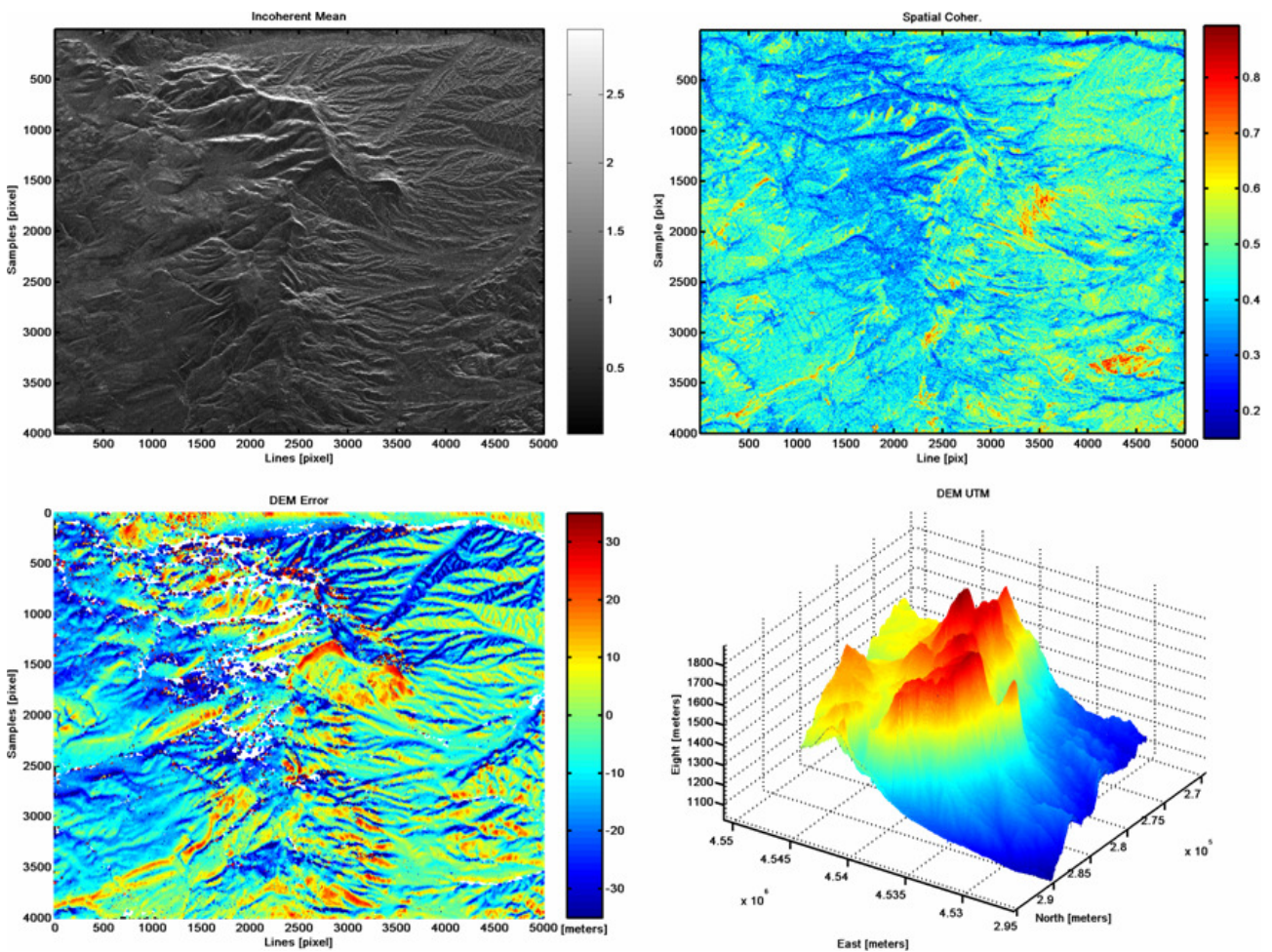


Figure 1. QPS processing results in the mountainous area around the city of Zhangbei. Top left: Incoherent mean of the dataset. Top right: averaged spatial coherence. Bottom left: height error in respect to the SRTM DEM. Bottom right: geocoded DEM (UTM coordinates)

3. GROUND DEFORMATION IN THREE GORGES AREA

Nowadays, China is dedicated to a large-scale infrastructures construction and the Three Gorges Project (TGP), the largest hydroelectric project in the world, is one of the most significant constructions in the country. The dam was proved to be stable, but its deformation still needs to be continuously monitored as well as its surrounding area. In fact, slope instability is responsible for the most widespread natural hazards in the Three Gorges, with landslides being a frequent phenomenon. The problem has been deeply treated in [8], consequently in this work we put our attention on a small area next to the dam in order to point out the effectiveness of the QPS technique in the localization and estimation of ground deformations. The exploited dataset is composed of 40 Envisat images of track 75, acquired from 2003 to 2009. The analyzed area is centered on a town near the dam, in front of the Yangtze river, and its reflective map is shown in Fig. 2.

On the top right of the scene can be recognized a big dike, main object of our investigation. The upper row of Fig. 3 presents the results of QPS technique.

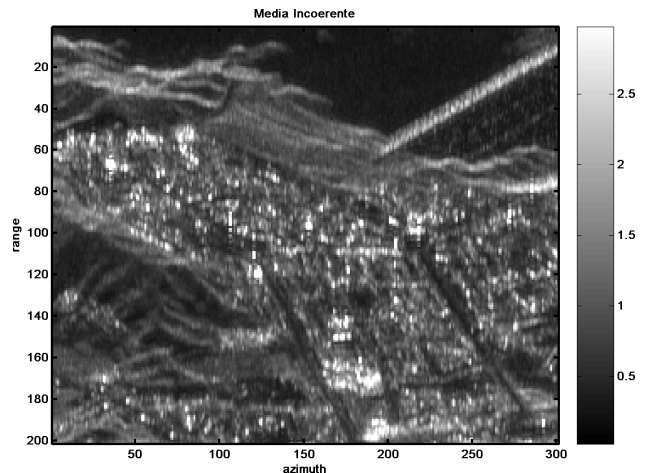


Figure 2. Incoherent mean of the analyzed area in the neighborhood of the Three Gorges Dam.

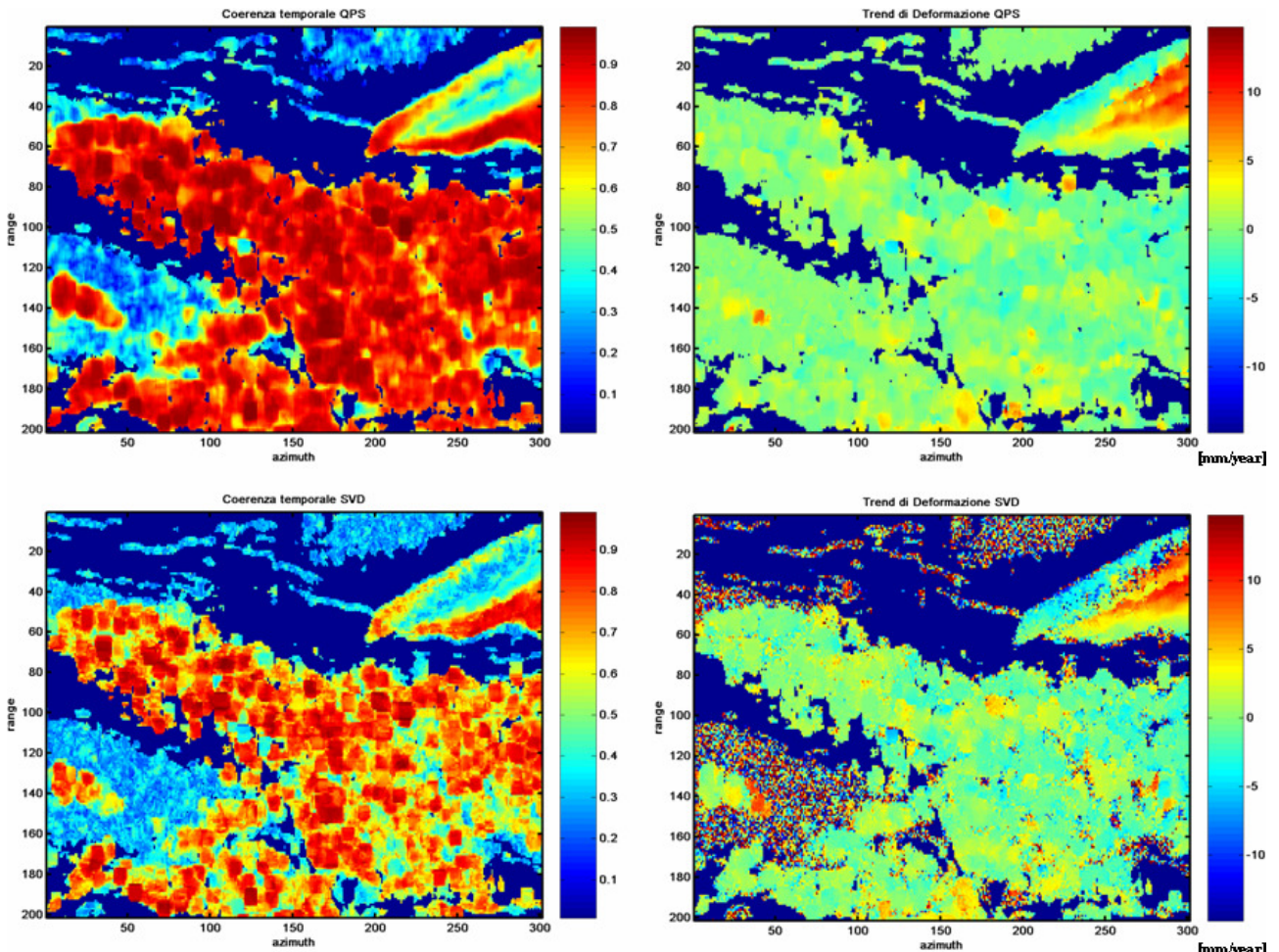


Figure 3. Time series analysis results on a small area next to the Three Gorges Dam. Top left panel: temporal coherence of the QPS analysis. Top right: deformation trends estimated by QPS technique. Bottom left panel: temporal coherence of the SVD analysis. Bottom right: deformation trends estimated by SVD technique.

The panel on the left shows the temporal coherence of the estimated deformation trends, which are displayed on the right. It can be noticed that the dike suffers of a deformation of several millimeters per year, due probably to the settlement after its construction.

In order to validate the QPS technique results, the same dataset has been processed with the SVD technique. Instead to use just the interferograms that connects at the best the images of the dataset as in the QPS technique, all the possible interferograms have been exploited by means of the singular value decomposition of the coherence matrices. After that, deformations trends can be easily retrieved for each point separately taking advantage of just the first SVD component. The results of this method are shown in the lower row of Fig. 3.

From the comparison of the deformation trends of the two techniques, it can be appreciated their high agreement. More in depth, the SVD technique, exploiting all the information at hand, allows a slight improvement in the resolution, but it costs a higher computational burden.

4. RAILWAYS MONITORING

In 2005 the high-speed railway system began being built in different locations in China. The planned system consists of four horizontal and four vertical main railways, which will connect the main metropolises in China. Compared with normal ones, high-speed railways require very high stability of the structures on which trains run with speed up to 400km/h. As a consequence, the displacement of railways needs to be carefully monitored. In literature some PS case studies along railways can be found (see e.g. [9, 10]).

We present the time series InSAR analysis results along a straight railway. The study area is located in the west part of the municipality of Shanghai. Fig. 4 shows the location of the study area and of the railway, which connects the city of Shanghai with the town of Kunshan, passing through the Jiading district.

On the studied area, 4 different swaths imaged by the radar in 4 different orbits are available. The number of images for each track is shown in Table 1.

Table 1: Archived datasets in different tracks.

Track #	Ascending / Descending	ERS-1 #	ERS-2 #	ENVISAT #
268	A	-	-	14
497	A	-	-	12
275	D	-	-	9
3	D	17	26	11

In Fig. 5 we show a detail of the reflectivity map of the 4 datasets at hand. Each map represent the same

area under different geometries with, at the centre of the scene, a piece of the railway under analysis. From Fig. 5 it's evident the dependence of the visibility of the railway with the satellite acquisition geometry: the linear target is clearly visible, with high amplitude values, in correspondence of the Track 3 dataset.



Figure 4. Test site in Shanghai

Fig. 6 shows on the left part another detail of the reflective map of Track 3 centred on a straight stretch of the railway and, on the right side, the amplitude mean calculated along the range direction. It's possible to observe the two amplitude peaks corresponding to the tracks of the railway. In the following we concentrate our attention on the 43 ERS-1/2 SAR images acquired on Track 3.

In order to monitor a railway by means of InSAR time series analysis, we can distinguish two cases: in the first one the structural details of the railway and its inclination allow the radar to directly monitor the structure itself, in the other one the stability of tracks can be in first approximation derived by the motion of surrounding targets. In the second case, whenever the surrounding area is extra-urban and thus poor of PSs, two possible research directions are here addressed: 1) improving the target density by considering also partially coherent targets. 2) In case of long linear rail tracks, exploiting the linearity of the structure to enhance the interferometric coherence.

The dataset under study has been acquired during 1990s. In those years the analyzed area was not urbanized and agricultural fields can be observed from the SAR images. To process the area, according to the first research topic, we made use of the QPS approach. Moreover, since the studied railway is straight, a one dimensional Coherence Estimation Window (CEW) has been used to separate the signal of the railway from the surrounding noise, according to the consistence of interferometric phase along the railway.

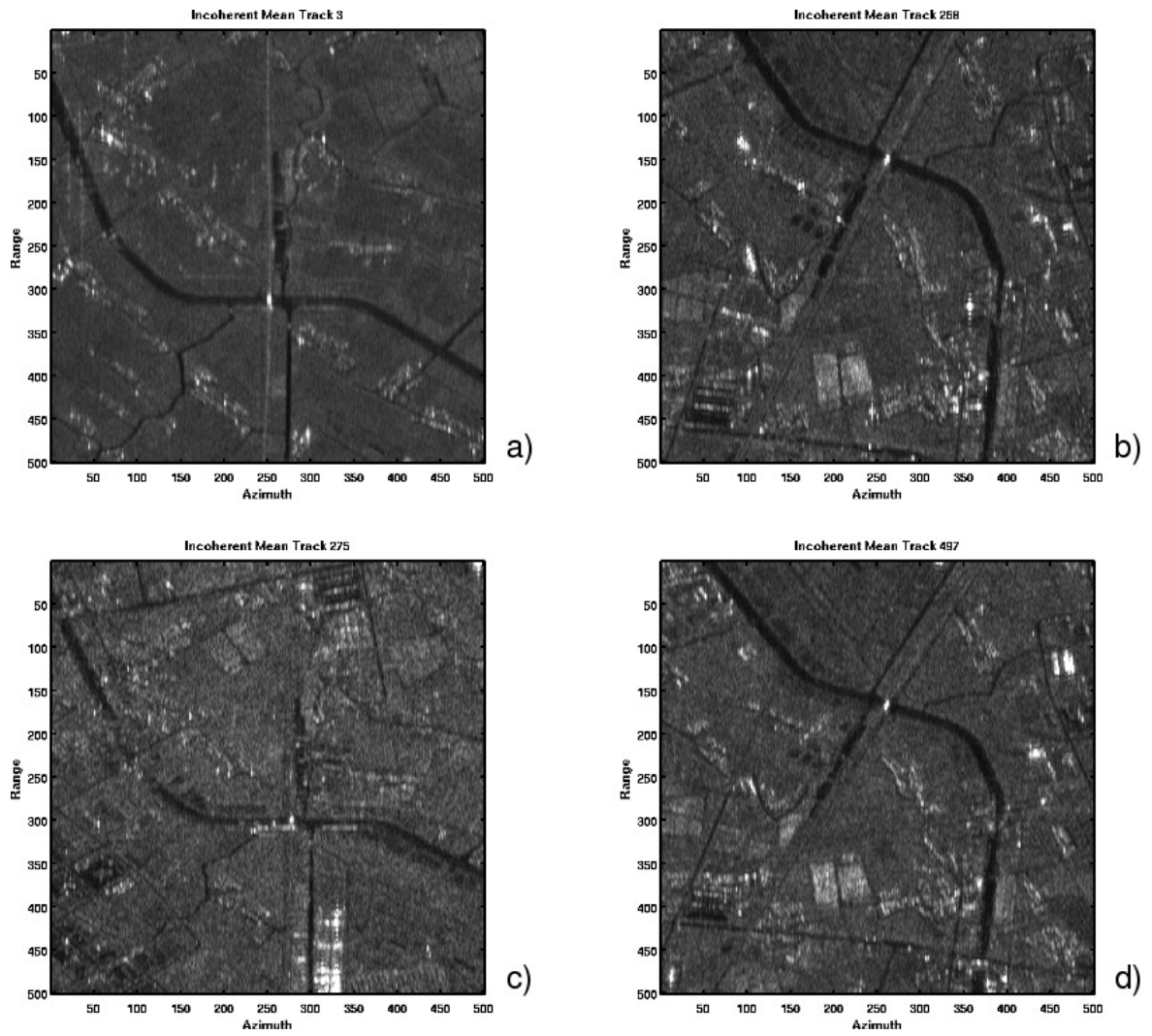


Figure 5. Detail of the reflective maps of the 4 datasets of the Shanghai area , namely (a) (b) (c) (d), referred to Track 3,Track 268, Track 275, Track 497.

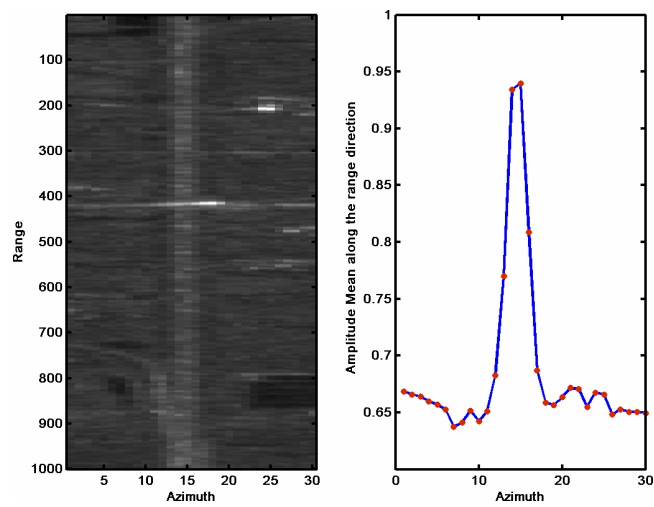


Figure 6. Left: resampled Track 3 reflective map (detail). Right: amplitude mean along the range direction

4.1. QPS Analysis

Fig. 7 collects the main results of the QPS analysis. In the first image on the left, the amplitude map along the railway is shown. For the sake of visualization, the horizontal scale has been magnified by a factor of 2. Fig. 5 (b) shows the PSC candidates selected by analyzing the amplitude series, from which the straight line of the railway can be seen. The temporal coherence estimated by the QPS technique is shown in (c). Although the original PS technique failed to detect coherent targets in this area, by means of the QPS, 5104 points in 20 km² with temporal coherence higher than 0.75 were found.

As we mentioned in the previous section, in the 1990s, the test site was still un-urbanized. In fact, comparing Fig. 5(a) with the other 3 reflectivity maps (b,c,d), the bright targets are much fewer. Nevertheless, the density of the detected QPS is still high enough to measure the subsidence of the area. Since the deformation along the railway will be hidden by plotting the estimated deformation trends on all points, only QPS with strong subsidence rates are shown in Fig. 7 (d). Along the railway, some abnormal deformation trend can be

found on some points. By investigating the test site, a small train station can be found in the middle of the railway, where some QPS with heavy subsidence are identified. In Fig. 5 (e), the subsidence map interpolated with a standard Kriging process along the railway is shown. Areas plotted with red colour indicates the detected subsidence. Thus, the time series analysis can offer a good and cheap methods to locate possible risk areas. The result can be used to drive the placement of GPS receivers to study the deformation in time.

4.2. Coherence Analysis

A railway is a complicated target formed by a set of different parts like rails, sleepers, poles and the track ballast, but the ensemble of these elementary targets is aligned along the same direction. Thus, a possible model of a railway is that of a uniform and distributed target aligned along a main direction. This hypothesis can be investigated by means of a coherence analysis carried out on the interferogram stacks.

Let us denote with s_i the i -th complex SAR image

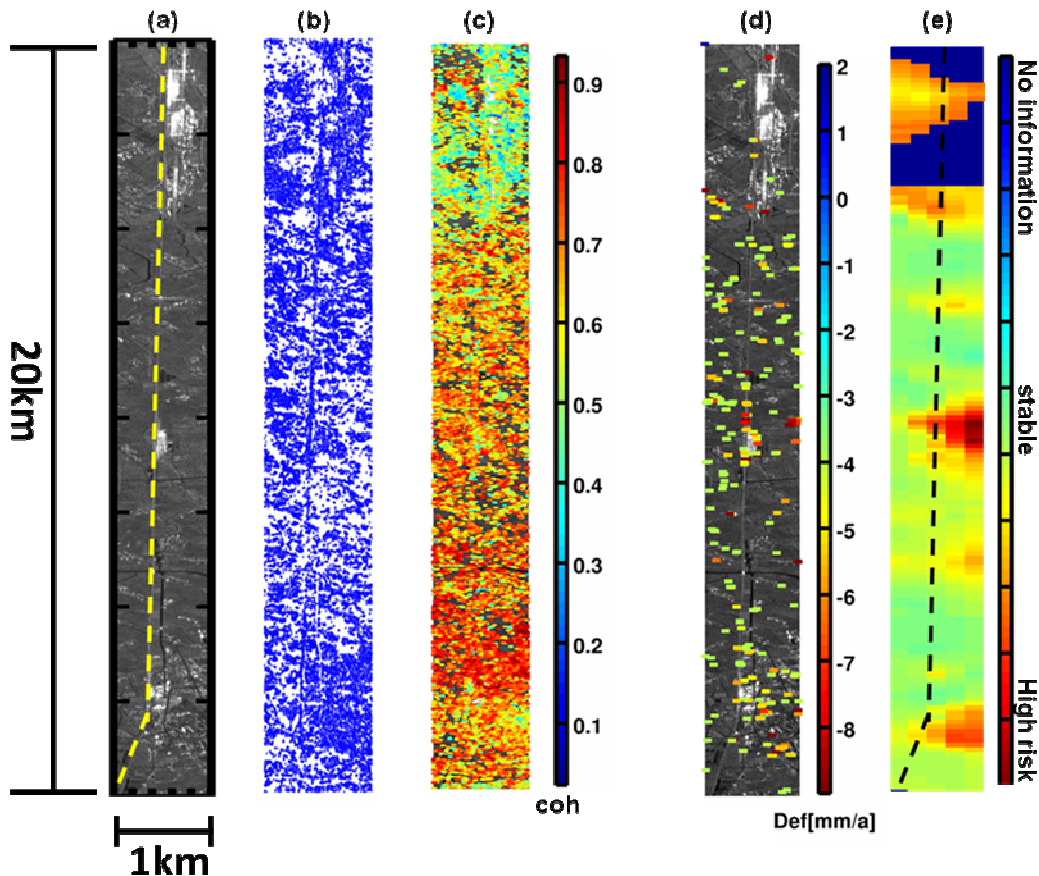


Figure 7. QPS processing results. (a) reflective map, (b) QPS candidates, (c) temporal coherence, (d) QPS with high subsidence trends (e) Kriging interpolated deformation fields, the red areas indicate high risk subsidence regions along the railway.

(with $i, j = 1 \dots N_I$). The interferogram between the images i and j can thus be expressed as $I_{i,j} = s_i \cdot s_j^*$.

The spatial coherence $\gamma_p^{i,j}$ of each point p of each interferogram $I_{i,j}$ is retrieved as the normalized cross-correlation coefficient between the two images i, j over an appropriate $CEW(p)$:

$$\gamma_p^{i,j} = \frac{\sum_{CEW(p)} I_{i,j}}{\sqrt{\sum_{CEW(p)} |s_i|^2 \sum_{CEW(p)} |s_j|^2}} \quad (1)$$

Within our test site, the straight railway is composed by two different parallel tracks aligned in a direction that differs from the radar slant range direction of an angle less than 1 degree. According to the shape of the railway, a one-pixel wide (4m) CEW is selected, 500m long along the railway direction. In this way, we try to keep separated the two adjacent railway tracks.

To highlight the intrinsic coherence of a railway with respect to the surrounding area, it is useful to compare it with the coherence estimated along different directions. In particular, we choose to rotate the CEW angle between -10 and +10 deg. Given the point p on the railway (with $p = 1 \dots N_p$), we define $\gamma_p^{i,j}(\vartheta)$ as the coherence of the interferogram $I_{i,j}$ along the $CEW(\vartheta)$ centred on point p .

As result, we show in Fig. 8 the absolute value of the coherence averaged on all the pixels of the railway and with the changing ϑ expressed by:

$$\bar{\gamma}(\vartheta) = \frac{1}{N_{UP(I)}} \frac{1}{N_p} \sum_{UP(I)} \sum_p |\gamma_p^{i,j}(\vartheta)| \quad (2)$$

where $UP(I)$ is the set of the 25% most coherent interferograms and $N_{UP(I)}$ is the number of $UP(I)$.

The result shows how the temporal coherence has the highest value in correspondence of the railway and decreases when we rotate the CEW. According to [11], SAR interferometric coherence can be mainly decomposed into geometric and temporal contributions. Consequently, in the following discussions, the de-correlation of the railway is investigated in these two domains.

With our coherence analysis, a covariance matrix [12] is estimated for each pixel along the railway and under different $CEW(\vartheta)$. Since each matrix represents the correlation properties in a particular place in the scene, to resume the coherence of the whole railway compared to the surrounding areas we

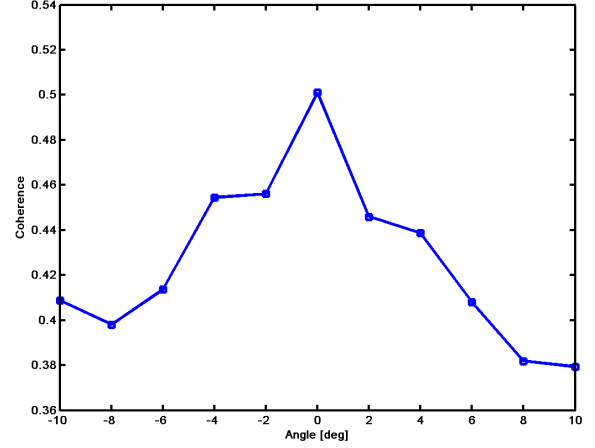


Figure 8. Mean coherence estimates with different angles. The highest coherence estimate is obtained along the railway.

can average the absolute values of all matrices with respect to a $CEW(\vartheta)$:

$$\bar{\gamma}^{i,j}(\vartheta) = \frac{1}{N_p} \sum_p |\gamma_p^{i,j}(\vartheta)| \quad (3)$$

As a result, we present Fig. 9 the averaged covariance matrices for $\vartheta = 0^\circ$ (CEW is aligned with the railway) and $\vartheta = -8^\circ$. The images are arranged by the acquisition date and each element in the matrix represents the coherence of the corresponding interferogram. The principal diagonal is unitary because every image is perfectly coherent with itself.

From the comparison of this two matrices it is easy to notice that there exist a subset of interferograms in which the matrix calculated on $CEW(0^\circ)$ has higher coherence. It is interesting to notice that some of these interferograms also have quite high temporal baselines, instead to be just near the principal diagonal. This extend the de-correlation time of the railway with respect to the surrounding area. Posing a threshold of 0.5, on the railway we can obtain coherent interferograms also between two acquisitions distant 350 days one from each other. On the contrary, in the neighbourhood such coherence is present with temporal baselines of maximum 70 days. This experimental result bears out the hypothesis of high temporal stability of the railway.

It is of interest looking at the same results of Fig. 9 from the normal baseline dimension viewpoint. In Fig. 10 the coherence values of the two matrices in Fig.9 are displayed dependent on the normal baseline. The goodness of the interferograms has a strong dependence on this dimension because of the spectral shift that causes a linear-like decrease of the coherence. Moreover it's possible to noticed that values are near to

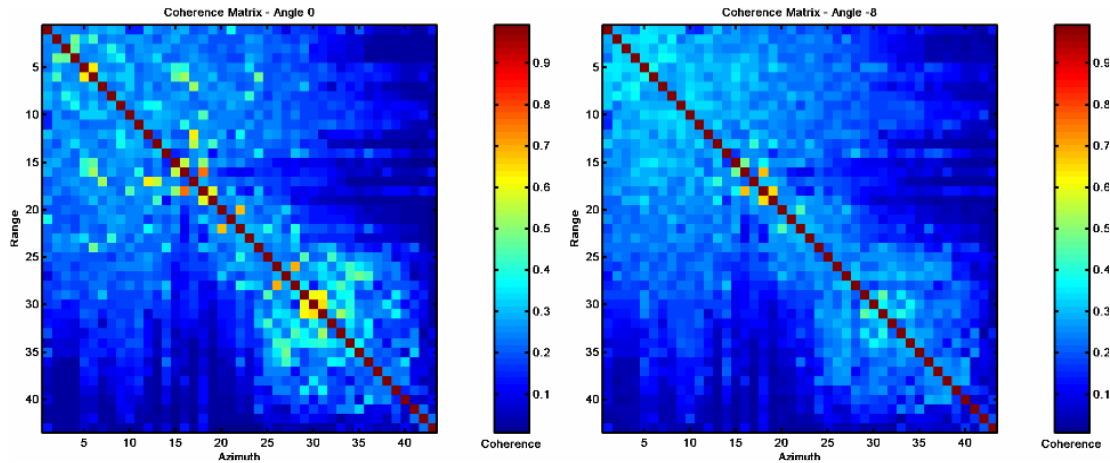


Figure 9. Coherence matrices ordered with respect to temporal baselines. Left: calculated on a linear window along the railway. Right: CEW oriented in a different direction.

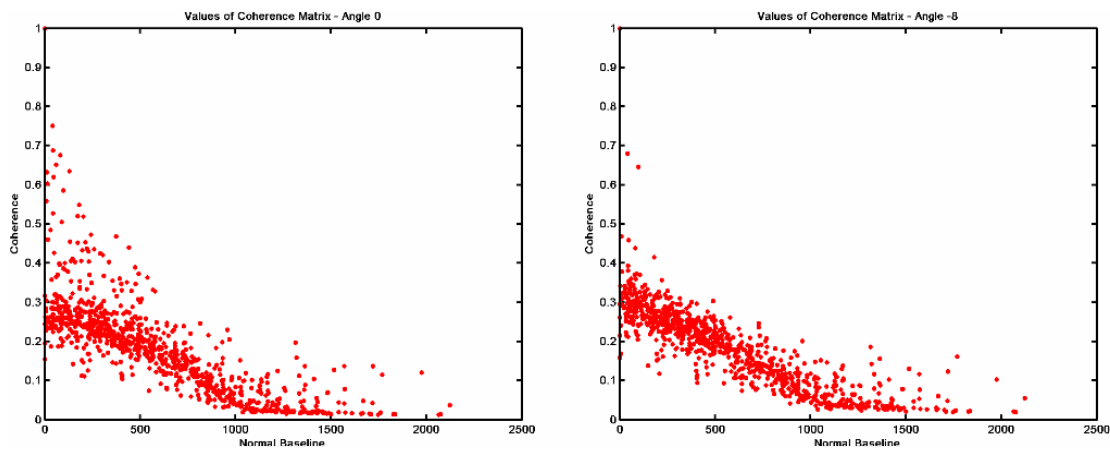


Figure 10. Coherence matrices values of Fig. 9 ordered with respect to normal baselines.

zero with a normal baseline larger than 1000 – 1100 m, which is the ERS critical baseline. This effect, due to the geometric de-correlation, is in agreement with the structure of the railway under analysis, that is not exactly a linear target, but a complicated structure formed by the composition of a set of punctual targets aligned along a main direction.

Furthermore, also from Fig. 10 we can extract the information of the presence of a subset of interferograms with much higher coherence in correspondence of the railway compared to the surrounding area values. This subset, represented by the outliers from the pseudo-linear distribution, is confined to the low baseline region (smaller than 500m).

5. CONCLUSIONS

Nowadays China is in an era of rapid urban development. Large-scale infrastructure as Three Gorges Dam or high-speed railway system needs to be precisely and regularly monitored, in order to prevent risks due to ground deformations like landslides or subsidences. SAR Interferometry has proved to be a

suitable tool to solve the problem at hand. In particular, the main aim of this work is to show the potentiality of QPS technique, especially in un-urbanized areas.

From the obtained results, time series InSAR analyses show being able to estimate height errors with respect to an a-priori DEM and to identify subsiding areas. Consequently it offers a good and cheap method to locate possible risk areas. As a second step, the result can be used to drive the placement of GPS receivers to study the deformation in time.

Moreover, a coherence analysis has been carried out on the interferometric stacks. Since the railway is formed by a set of elementary targets aligned along the same direction, a one-dimensional CEW is proposed. According to our results, the coherence of the railway keeps high values in long temporal baseline interferograms with respect to the surrounding targets. The proposed linear CEW also improves the spatial coherence estimation and shows the potential coherent information along railways. As future work, the same procedures can be used to select the subset of interferograms with highest coherence.

6. REFERENCES

- [1] Ge, D.; Wang, Y.; Zhang, L.; Wang, Y. and Hu, Q.; "Monitoring urban subsidence with coherent point target SAR interferometry," *Urban Remote Sensing Event*, 2009 Joint, 2009, pp. 1-4.
- [2] Ferretti, A.; Prati, C.; Rocca, F., "Permanent scatterers in SAR interferometry," *IEEE Transactions on Geoscience and Remote Sensing*, vol.39, no.1, pp.8-20, Jan 2001
- [3] Ferretti, A.; Savio, G.; Barzaghi, R.; Borghi, A.; Musazzi, S.; Novali, F.; Prati, C. and Rocca, F.; "Submillimeter Accuracy of InSAR Time Series: Experimental Validation," *IEEE Transactions on Geoscience and Remote Sensing*, vol. 45, pp. 1142-1153, 2007.
- [4] Perissin, D.; "Validation of the Sub-metric Accuracy of Vertical Positioning of PS's in C Band," *IEEE Geoscience and Remote Sensing Letters*, vol.5, pp. 502-506, 2008.
- [5] Perissin, D.; "SAR super-resolution and characterization of urban targets," *PhD Thesis, Dipartimento di Elettronica e Informazione, Politecnico di Milano*, 2006.
- [6] Perissin, D.; Ferretti, A.; Piantanida, R.; Piccagli, D.; Prati, C.; Rocca, F.; De Zan, F. and Rucci, A.; "Repeat-pass SAR Interferometry with Partially Coherent Targets," *ESA Fringe 07*, Frascati, Italy, 2007.
- [7] Wang, T.; Perissin, D.; Liao, M. and Rocca, F.; "Deformation Monitoring by Long Term D-InSAR Analysis in Three Gorges Area, China," *Geoscience and Remote Sensing Symposium, IGARSS 2008*, pp. IV-5 – IV-8, 2008.
- [8] Wang, T.; Tang, J.; Liao, M.; Perissin, D.; Balz, T.; Zhang, L.; "Landslides Monitoring over the Three Gorges Region with C- and X-band InSAR data," *ESA Dragon 2 Mid Term Result Publication*, 2010.
- [9] Ge, D.; Wang, Y.; Guo, X.; Wang, Y.; Xia, Y.; "Land Subsidence Investigation Along Railway Using Permanent Scatterers SAR Interferometry," *Geoscience and Remote Sensing Symposium, IGARSS 2008*, pp. II-1235 – II-1238, 2008.
- [10] Xie, C.; Li, Z.; Li, X.; "A Permanent Scatterers Method for Analysis of Deformation over Permafrost Regions of Qinghai-Tibetan Plateau," *Geoscience and Remote Sensing Symposium, IGARSS 2008*, pp. IV-1050 – II-1053, 2008.
- [11] Wang, T.; Liao, M. and Perissin, D.; "Coherence Decomposition Analysis," *IEEE Geoscience and Remote Sensing Letters*, vol. 7, pp. 156-160, 2010.
- [12] Rocca, F.; "Modeling Interferogram Stacks," *IEEE Transactions on Geoscience and Remote Sensing*, vol. 45, pp. 3289-3299, 2007.